PHYSICAL REVIEW B, VOLUME 65, 104509

Localization by disorder in the infrared conductivity of $Y_{1-x}Pr_xBa_2Cu_3O_7$ films

R. P. S. M. Lobo*
Laboratoire de Physique du Solide, Ecole Supérieure de Physique et Chimie Industrielles de la Ville de Paris, CNRS UPR 5, 75231 Paris Cedex 5, France

E. Ya. Sherman
Institute für Theoretische Physik, Karl-Frazens-Universität, A-8010, Graz, Austria

D. Racah and Y. Dagan
Department of Physics and Astronomy, Tel-Aviv University, Ramat-Aviv, Tel-Aviv, 69978 Israel

N. Bontemps
Laboratoire de Physique du Solide, Ecole Supérieure de Physique et Chimie Industrielles de la Ville de Paris, CNRS UPR 5, 75231 Paris Cedex 5, France

(Received 5 April 2001; published 14 February 2002)

The *ab*-plane reflectivity of $(Y_{1-x}Pr_x)Ba_2Cu_3O_7$ thin films was measured in the 30–30 000 cm^{-1} range for samples with $x=0$ ($T_c=90$ K), $x=0.4$ ($T_c=35$ K), and $x=0.5$ ($T_c=19$ K) as a function of temperature in the normal state. The effective charge density obtained from the integrated spectral weight decreases with increasing *x*. The variation is consistent with the higher dc resistivity for $x=0.4$, but is one order of magnitude smaller than what would be expected for $x=0.5$. In the latter sample, the conductivity is dominated at all temperatures by a large localization peak. Its magnitude increases as the temperature decreases. We relate this peak to the dc resistivity enhancement. A simple localization-by-disorder model accounts for the optical conductivity of the $x=0.5$ sample.

DOI: 10.1103/PhysRevB.65.104509 PACS number(s): 74.25.Gz, 74.76.Bz, 72.15.Rn

I. INTRODUCTION

The only consensus on the electronic properties of the normal state of high-T_c superconductors is that they are not conventional. Examples of models describing cuprates normal state are charge stripes,[1] polarons,[2,3] and various flavors of modified Fermi liquid[4–7] and Luttinger liquid.[8] All these models assume a strong electron-electron and/or electron-phonon interaction. The disorder introduced by cationic or oxygen doping influences the spectrum of excitations, making the physics of the system more complex. Indeed, Basov *et al.*[9] propose that the Drude-like peak observed in the infrared spectra of irradiated $YBa_2Cu_3O_7$ (YBCO) moves up in frequency to a localized state. Problems that have been discussed now for many years are the relevance of disorder to localization and localization to superconductivity, in particular near the metal-insulator transition.[10–12] In cuprates, this could apply to a strongly underdoped material. Another twist appears with the observation of a normal-state gap in underdoped cuprates.[13–16] It was first observed as a pseudogap in NMR data.[17] It was later associated with the departure from linearity in the resistivity.[15,16] Puchkov and co-workers[13] proposed that the apparent optical conductivity spectral weight loss in the normal state of underdoped cuprates is a manifestation of the pseudogap.

There is a significant (and somewhat contradictory) body of literature suggesting both hole depletion in the CuO_2 planes and localization in Pr-substituted compounds.[18–26] In this paper we describe the optical reflectivity of Pr-doped $YBa_2Cu_3O_7$ (Pr-YBCO) *ab*-plane thin films as a function of temperature.

The optical conductivity of untwinned single crystals of nonsuperconducting $PrBa_2Cu_3O_7$ (PBCO) shows that substitution of Y by Pr empties the CuO_2 planes and localizes the charges into a midinfrared band presumably along the CuO chains.[27] Optical (Ref. 28) ($x\leqslant 0.35$) and coherent THz (Ref. 29) ($x\leqslant 0.4$) data on the in-plane response of Pr-YBCO support a picture in which the localization grows continuously with Pr doping. More recently, Bernhard and co-workers measured the far-infrared *c*-axis conductivity of Pr-YBCO using ellipsometry. Their data suggest that Pr acts as an underdoping agent.[30] For their highest doping ($x=0.45$) they find some indirect support of charge localization. However, a localization peak has not been resolved in Pr-YBCO.

We investigate $Y_{1-x}Pr_xBa_2Cu_3O_7$ samples with $x=0$, 0.4, and 0.5. The superconducting state of the first two compositions is discussed in detail elsewhere.[31] In this paper we resolve the localization peak in Pr-YBCO at the composition $x=0.5$. A simple localization model based on Pr disorder reproduces this localization peak. We suggest that a signature of this peak is already present in the $x=0.4$ compound and competes with the normal-state gap opening.

II. EXPERIMENT

Thin films of pure and Pr-doped $YBa_2Cu_3O_7$ were grown by sputtering on stabilized zirconia (YSZ) substrates. The samples are *c*-axis oriented and typically 5000 Å thick. The four-point electrical dc resistivity is shown in Fig. 1, giving $T_c=90$ K ($x=0$), $T_c=35$ K ($x=0.4$), and $T_c=19$ K ($x=0.5$). The resistivity of the $x=0.5$ compound is almost an order of magnitude higher (right-hand side scale) than that of

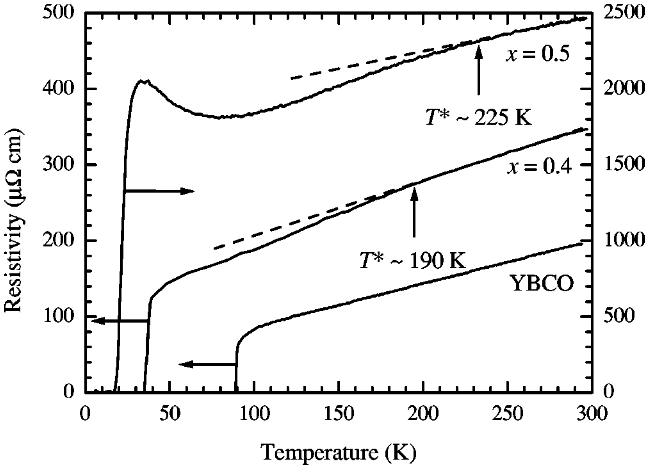

FIG. 1. Temperature dependence of the dc resistivity of (Pr,Y)$Ba_2Cu_3O_7$ films on YSZ. Note that the $x=0.5$ compound (right-hand axis) is almost one order of magnitude more resistive than $x=0.4$ and pure YBCO. The temperature where the resistivity no longer shows a linear thermal dependence is indicated by T^*.

pure or $x=0.4$ Pr-YBCO (left-hand side scale). The dashed straight lines help to locate approximately the pseudogap opening temperature (T^*) in the Pr-doped samples, indicated by the arrows. Note that in the $x=0.5$ compound an upturn before the superconducting transition occurs. One relevant point to this work is that similar T^*'s can be seen in underdoped YBCO films[15] having T_c's of 70 K and 60 K.

Our infrared reflectivity spectra were obtained with a Bruker IFS 66v interferometer between 30 and 7000 cm^{-1}. A 4 K bolometer was used to take data up to 500 cm^{-1} and a DTGS/KBr pyroelectric detector was used in the midinfrared. Near-infrared and visible data between 4000 and 30 000 cm^{-1} were measured in a Cary 4000 grating spectrometer with a photomultiplier. In the overlapping spectral range, measurements from both spectrometers agree within 0.5%. We used gold mirrors as a reference for measures in the Bruker spectrometer and silver mirrors in the Cary. We utilized a He gas flow cryostat to measure the spectra between 6 K and room temperature in the whole frequency range. The temperature stability during the measurements was better than 0.5 K. Polypropilene (far-infrared and visible) and ZnSe (midinfrared) windows were used to cover the whole spectral range.

III. DATA ANALYSIS

The spectral functions were determined for our samples by Kramers-Kronig transform. At low frequencies (below 30 cm^{-1}) a Hagen-Rubens extrapolation was used at all temperatures, including the superconducting state. Above the highest measured frequency (30 000 cm^{-1}) the reflectivity was assumed to be constant up to 10^6 cm^{-1} followed by a ω^{-4} termination to infinity. Below 150 K our samples are opaque enough to avoid a significant contribution from the substrate. We also checked that different low-frequency extrapolations do not change the conductivities more than 7% at 100 cm^{-1} and not more than 2% at 200 cm^{-1}. Above 250 cm^{-1} the differences are negligible.

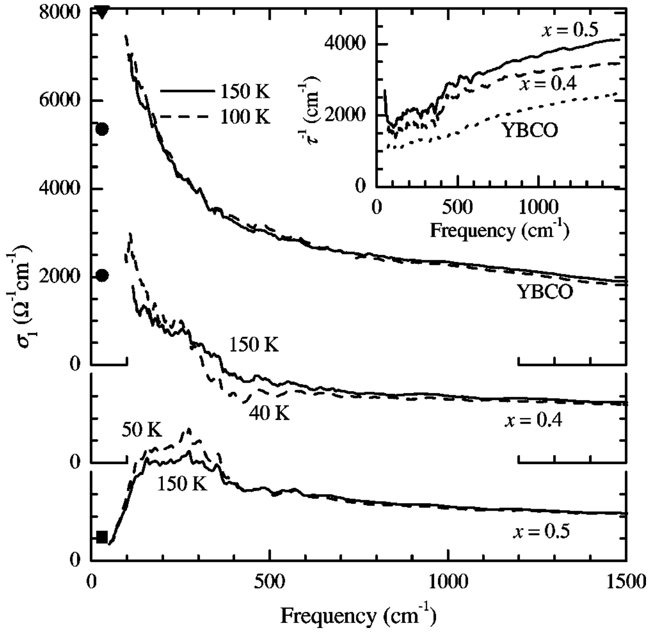

FIG. 2. Real part of the optical conductivity of Pr-YBCO films on YSZ. From top to bottom $x=0$, 0.4, and 0.5. The solid symbols are obtained from the dc resistivity for the corresponding temperatures in the normal state. In the $x=0.5$ sample σ_1 is dominated by a peak around 300 cm^{-1}. The inset shows the scattering rate at 100 K for all samples. The scales for the $x=0.4$ and 0 conductivities are shifted with respect to the $x=0.5$ sample by 2000 and 4000 Ω^{-1} cm^{-1}, respectively.

A generalization of the Drude model can be obtained using a frequency-dependent scattering rate[32,33] defined as

$$\frac{1}{\tau}=\frac{2\pi}{Z_0}\Omega_p^2\frac{\sigma_1}{\sigma_1^2+\sigma_2^2}, \tag{1}$$

$Z_0=377$ Ω being the vacuum impedance. Ω_p, the effective plasma frequency, is related to the charge density n, carrier effective mass m^*, and vacuum permittivity ϵ_0 by $\Omega_p^2=ne^2/\epsilon_0 m^*$.[34] Here $\sigma(\omega)=\sigma_1+i\sigma_2$ is the complex conductivity.

One can estimate the plasma frequency through the classical sum rule

$$\Omega_p^2=\frac{Z_0}{\pi^2}\int_0^\infty \sigma_1(\omega)d\omega. \tag{2}$$

One usually introduces a cutoff energy (1–2 eV) in order to restrict the integration to the free carrier contribution. Equations (1) and (2) assume that Ω_p, τ^{-1}, and ω are measured in cm^{-1} and σ_1 in Ω^{-1} cm^{-1}.

IV. RESULTS

Figure 2 shows the real part of the optical conductivity for all three samples: $x=0$, 0.4, and 0.5. The normal-state low-frequency conductivity extrapolates consistently at various

TABLE I. Pr-YBCO characteristic parameters. T_c and ΔT_c (in parentheses) are directly obtained from the resistivity in Fig. 1. Ω_p and N_{eff} are obtained with Eq. (2) integrating the room-temperature optical conductivity up to 1.5 eV. N_{eff} uses the bare electron mass as m^*. α is the slope of the linear part of the resistivity (dashed lines in Fig. 1).

x	T_c(K)	Ω_p (cm^{-1})	N_{eff} (cm^{-3})	$\alpha(\mu\Omega$ cm/K)
0	89(1)	22000	5.1×10^{21}	0.57
0.4	35(2.5)	19200	4.1×10^{21}	0.72
0.5	19(7)	18000	3.6×10^{21}	2.3

temperatures to the measured dc conductivity (solid symbols).

The YBCO film exhibits a conventional behavior. Its spectral response does not change significantly in the normal state from 150 K to 100 K and is dominated by a Drude-like peak. YSZ is not the best substrate to grow YBCO. For instance, the residual conductivity in the superconducting state is twice as high as that from the best films.[31] However, our YBCO's normal-state conductivity and scattering rate are qualitatively and quantitatively the same as those from good samples.[13]

In the $x=0.4$ film the free carrier response is still the major contribution to the normal-state conductivity. The loss of spectral weight from $\sim$800 cm^{-1} down to 300 cm^{-1} observed at temperatures above T_c is assigned to the opening of the normal-state gap.[31] It is worth remarking at this point that a weak shoulder appears at 250 cm^{-1} in the 40 K spectrum.

A major change, consistent with the huge increase in the dc resistivity, is observed in the $x=0.5$ sample. The free carrier contribution is not seen and is replaced by a broad peak centered around 250 cm^{-1} that dominates the far-infrared spectrum (below 700 cm^{-1}). These spectra do not show any signature of a pseudogap or of the superconducting transition. Actually, an opposite effect is observed since the magnitude of the peak around 250 cm^{-1} increases with decreasing temperature.

In the inset we show the frequency-dependent scattering rate calculated with Eq. (1). The YBCO film displays a standard behavior with a scattering rate $1/\tau$ depending roughly linearly on frequency in the normal state. In the Pr-substituted samples the absolute value of $1/\tau$ increases and some structures appear at low frequencies (250 cm^{-1}). Both effects indicate a lower mobility of charge carriers with a possible localization effect.

The values for Ω_p estimated from the conductivity integrated up to 1.5 eV at $T=300$ K are shown in Table I. The charge carrier concentration N_{eff} is derived from Ω_p assuming that m^* is the bare electron mass. In Fig. 3, we display the thermal evolution of N_{eff} for each sample normalized by its value at 300 K. The estimated error in N_{eff} is about twice the symbol size. The arrows indicate the measured T_c. All samples exhibit a decrease of the carrier density when crossing T_c, associated with the spectral weight transferred to the zero-centered δ function. The inset shows the same data normalized by N_{eff} of YBCO at 300 K for all samples.

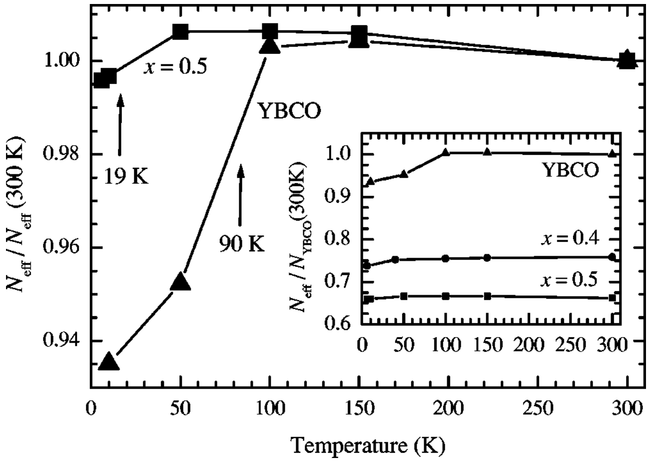

FIG. 3. Thermal dependence of the charge density (normalized to its value at 300 K) calculated with Eq. (2) integrated up to 1.5 eV. The arrows indicate the critical temperature for each sample. The estimated error in N_{eff} is roughly twice the symbol size. The inset shows the same data, now normalized for all samples to the effective charge of YBCO at 300 K.

V. DISCUSSION

Even though there are not many data points in Fig. 3, we can infer some general trends for each sample. In pure YBCO we observe that, within experimental error, N_{eff} does not vary in the normal state. In the $x=0.5$ sample N_{eff} increases when cooling down to 50 K and then begins decreasing. The increase is consistent with the accumulating spectral weight in the low-frequency peak. The decrease at low temperatures is the signature of the superconducting transition.

The $x=0.5$ Pr sample exhibits a clear peak at $\sim$250 cm^{-1}. Experiments in YBCO and pure PBCO have shown a peak in the conductivity when light is polarized along the b axis.[27,35] In pure PBCO, the peak at an energy $\sim$1700 cm^{-1} has been assigned to localized carriers in the chains.[27] In single-domain YBCO crystals, the b-axis conductivity displays a peak at $\sim$300 cm^{-1}, again assigned to the chains.[35] Other authors did suggest disorder on Pr sites or in oxygen environment.[22,36] Two-dimensional (2D) localization within the CuO$_2$ planes has also been proposed.[24,36] Localization by disorder is notorious in (superconducting) samples.[37–39] Similar peaks have already been observed in high-T_c compounds,[40–42] some of them being purposely disordered.[9,41] Therefore, we propose to assign this peak to states localized by disorder in our samples, whether in the chains or in the planes.

The influence of Pr ions located between the cuprate planes on the energy of the electronic states in their vicinity has two different reasons. First, Pr changes the energy of the carriers in each CuO$_2$ plane. Second, Pr changes the electron hopping matrix element between the planes since the hopping occurs via either Y or Pr orbitals. Due to the hopping, the wave functions of the electronic states are either even or odd with respect to the reflection in the Y/Pr plane. The electronic density of the odd states vanishes at the Y/Pr plane, and, therefore, Pr influences the even and odd states differently. Localization in the planes can be described by a simple quantum-mechanical model, a shallow 2D potential well of radius a and depth U_0:

$$U(\rho)=\begin{cases}-U_0, & \rho<a,\\ 0, & \rho\geqslant a,\end{cases}\qquad \frac{\hbar^2}{m^*a^2}>U_0, \tag{3}$$

where ρ is the in-plane distance. Equation (3) implies that Pr ions modify in their vicinity the effective crystal potential acting upon the carriers. Therefore, $2a$ is expected to be close to the lattice parameter in the $\mathrm{CuO_2}$ plane, while U_0 depends on the parity of the state. The depths of the well should be typically of the order of 1 eV due to a relatively large difference between Pr and Y ions. However, due to the two dimensionality of the system, this potential yields a weakly bound state with energy $-\varepsilon_0 \ll U_0$:

$$\varepsilon_0=-\frac{2\hbar^2}{m^*a^2}\exp\left(-\frac{2\hbar^2}{m^*a^2}\frac{1}{U_0}\right), \tag{4}$$

with the Fourier component of the wave function

$$\psi(q)=2\sqrt{\pi}\frac{l}{1+l^2q^2}, \tag{5}$$

where the radius of the bound state is $l=\hbar/\sqrt{2m^*|\varepsilon_0|}\gg a$. An external electric field $\mathbf{E}=\mathbf{E}_0e^{-i\omega t}$ ($\mathbf{E}_0$ being the field amplitude) at the frequency $\omega\geqslant-\varepsilon_0/\hbar$ causes transitions from the localized to band states with momentum $p=\sqrt{2m^*(\hbar\omega+\varepsilon_0)}$. Using Fermi's golden rule, we obtain the transition rate (probability per time unit) from the $\psi(q)$ state to the band states:

$$W(\omega)=-2\pi\hbar\frac{e^2}{m^*}\varepsilon_0\frac{\hbar\omega+\varepsilon_0}{(\hbar\omega)^4}f_{\varepsilon_0}(1-f_{\varepsilon_0+\hbar\omega})E_0^2, \tag{6}$$

where f_{ε_0} and $f_{\varepsilon_0+\hbar\omega}$ are the filling factors of the states. Equation (6) assumes that the perturbation corresponding to the dipole interaction with the electric field is $\hat{V}=-i(e/m^*\omega)\hat{\mathbf{p}}\mathbf{E}$, $\hat{\mathbf{p}}$ being the momentum operator. The energy dissipation rate in a medium (per unity volume) is proportional to $\sigma_1(\omega)E_0^2$. In other words, the contribution of one localized state to $\sigma_1(\omega)E_0^2$ is proportional to the energy absorbed per transition multiplied by the transition rate. It then follows that the optical conductivity due to localized states is proportional to $W(\omega)$ in Eq. (6) multiplied by $\hbar\omega$ and the concentration of the localized states N_L. Neglecting the ω dependence of $f_{\varepsilon_0+\hbar\omega}$, the contribution of the localized states with the energy ε_0 to $\sigma_1(\omega)$ at $\omega\geqslant-\varepsilon_0/\hbar$ is then written as

$$\sigma_L(\omega)=-A\varepsilon_0\frac{\hbar\omega+\varepsilon_0}{(\hbar\omega)^3}, \tag{7}$$

where A is a constant proportional to the concentration of the bound states. At a temperature T a part of the localized states is empty due to thermal excitation, and the thermally activated carriers contribute in the Drude-like way to the optical conductivity. The localized states give the dominant contribution to $\sigma_1(\omega\sim|\varepsilon_0|/\hbar)$ if $N_L>N_0|\varepsilon_0|\tau/\hbar$ for $|\varepsilon_0|\tau/\hbar\gg1$ or $N_L>N_0\hbar/|\varepsilon_0|\tau$ for $|\varepsilon_0|\tau/\hbar\gg1$, where N_0 is the concentration of the mobile carriers participating in the Drude-like conductivity.

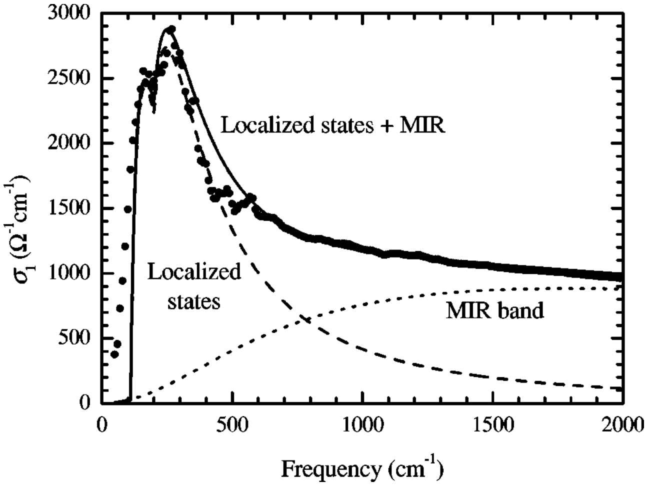

FIG. 4. IR conductivity at 50 K of the $x=0.5$ sample. The experimental data are the solid circles. The solid line is composed of two localization peaks and a mid-IR (MIR) peak. The individual contributions of the localization peaks are shown by the dashed line. The dotted line is the MIR contribution.

Virtually any conducting oxide shows a broad overdamped midinfrared band (MIB). Several papers attempted to describe this band in terms of various excitations such as polarons,[43–45] stripes,[46] two magnon,[47] etc. Nevertheless, no conclusive evidence to support any of this effects as being the MIB exists. For any practical purposes, it is widely accepted that the characteristics of the MIB (position and spectral weight) can be obtained from a Lorentz oscillator. Therefore, the general case for the conductivity composed of disordered and midinfrared states gives

$$\sigma_1(\omega)=\sum_{i=1}^{m}\sigma_L^{(i)}+\sum_{j=1}^{n}\frac{2\pi}{Z_0}\frac{\Delta\epsilon_j\Omega_{0(j)}^2\gamma_j\omega^2}{[\Omega_{0(j)}^2-\omega^2]^2+\gamma_j^2\omega^2}, \tag{8}$$

where the first summation is on disordered states and the second is the Lorentz MIR states.[48] $\Delta\epsilon$ is the oscillator strength, Ω_0 the resonance frequency, and γ its damping.

The solid circles in Fig. 4 show the conductivity of the $x=0.5$ sample at 50 K. Since the Pr substitution influences the odd and even states differently, one expects two different localization energies in the system, which correspond to contribution of the odd and even states in $\sigma_L(\omega)$. The solid line is a fit using the model in Eq. (8) with two disordered states[49] and one MIR oscillator. The fitting parameters are $|\varepsilon_0^{(1)}|=110\ \mathrm{cm^{-1}}$, $A^{(1)}=1.8\times10^6\ \Omega^{-1}\ \mathrm{cm^{-2}}$, $|\varepsilon_0^{(2)}|=200\ \mathrm{cm^{-1}}$, $A^{(2)}=1.5\times10^6\ \Omega^{-1}\ \mathrm{cm^{-2}}$, $\Delta\epsilon=90$, $\Omega_0=1800\ \mathrm{cm^{-1}}$, and $\gamma=5500\ \mathrm{cm^{-1}}$. Individual contributions from disordered localized states and MIR bands are shown, respectively, by dashed and dotted lines. The chosen values for $A^{(1)}$ and $A^{(2)}$ correspond to $N_L\sim10^{14}\ \mathrm{cm^{-2}}$ for odd and even states and m^* of the order of the bare electron mass. Going back to Eq. (4) we can estimate the radius of the potential well. Since $a\sim\sqrt{2}\hbar/\sqrt{U_0 m^{*}\ln(U_0/|\varepsilon_0|)}$, for $\varepsilon_0 \sim 200\ \mathrm{cm}^{-1}$(25 meV) and $U_0=1.0$ eV, we obtain a close to 2 Å. This radius of the potential well indicates that the changes really happen at the atomic level, consistent with our picture of disorder introduced by Pr ions.

Below 700 cm^{-1}, the IR conductivity shown in Fig. 4 is mostly described by this localization model. The model reproduces the amplitude and the asymmetric shape of the localization peak well.[50] The dc conductivity, however, is due to a small free carrier contribution.

Localization reconciles the apparent contradiction between the dc resistivity and the optical conductivity in the $x=0.5$ sample. The inset of Fig. 3 shows the behavior of the carrier density N_{eff} (normalized here to the 300 K YBCO value). The linear parts of the resistivity in Fig. 1 have their slopes shown in Table I. If Matthiessen's law were roughly followed, the ratio between slopes should be proportional to the ratio of the charge densities. The loss in spectral weight for $x=0.4$ follows satisfactorily the slope change observed in the dc measurements. The ratio between the resistivity slopes is 0.79 and the integrated charge density of the $x=0.4$ compound equals 76% that from YBCO. This suggests that what we observe here has to be mainly assigned to actual underdoping, namely a decrease of the ratio n/m^{*}.

A striking effect appears on the $x=0.5$ Pr sample. Whereas its dc conductivity is 5% of pure YBCO, the integrated carrier density is 65% of that from YBCO, entirely inconsistent with the observed resistivity increase. The slope ratio (0.24) is not of much help in solving this puzzle. We are thus led to conclude that the high dc resistivity in the $x=0.5$ sample is related to the localization of free carriers rather than to the decrease in their concentration. The Drude-like peak related to mobile charge carriers becomes a peak centered at 250 cm^{-1} without a strong loss of spectral weight.

Such a disorder induced localization must build up gradually with Pr concentration and localized states have to be present in the $x=0.4$ sample optical conductivity. The frequency-dependent scattering rate of the $x=0.4$ and $x=0.5$ samples shows similar structures around 250 cm^{-1}. At this very frequency, the optical conductivity of the $x=0.4$ material has a shoulder. Thus the localization peak is already present in the $x=0.4$ compound. Of course its oscillator strength is smaller and the mobile carriers response dominates the spectra[31] since the conditions $N_L > N_0|\varepsilon_0|\tau/\hbar$ or $N_L > N_0\hbar/|\varepsilon_0|\tau$ are not yet fulfilled there.

One may argue that substitution of Ba atoms by Pr would invalidate our model. However, Pr considerably replaces Ba only at very specific synthesis conditions forming crystals superconducting at 90 K.[51–54] This is clearly not the case in our films where Pr depletes superconductivity. We conclude therefore that our samples have Pr atoms in Y sites, in agreement with previous works.[18–31]

It is interesting to note that the loss of spectral weight in YBCO occurs at all frequencies below $\sim 800\ \mathrm{cm}^{-1}$.[13] Why then is the loss of spectral weight in the $x=0.4$ material limited to the 300–800 cm^{-1} range? According to the $x=0.5$ behavior, the localization peak evolves in the opposite direction of the normal-state gap. We suggest that the localization peak in the $x=0.4$ sample compensates the normal-state gap spectral weight loss in the 200 cm^{-1} region, thus explaining the apparent discrepancy between underdoped and Pr-substituted YBCO.

VI. SUMMARY

In summary, the optical response of Pr-YBCO films shows the localization of the charge carriers, thus clearly indicating the coexistence of localization and superconductivity. A peak in the optical conductivity due to this localization effect is fully resolved in the $x=0.5$ Pr-YBCO sample at 250 cm^{-1}. We argue that such a localization is already present in the $x=0.4$ sample and compensates the normal-state gap spectral weight loss. The localization peak is described through in-plane disorder introduced by Pr atoms.

ACKNOWLEDGMENTS

The authors are grateful to G. Deutscher and R. Combescot for helpful comments, and to B. Briat for his help with the visible measurements. One of us (R.P.S.M.L.) acknowledges financial support of UE Grant No. 93.2027.IL. E.Y.S. acknowledges support from the Austrian Science Fund via Project No. M591-TPH. This work was partially supported by the Oren Family chair of Experimental Solid State Physics.

---

*Present address: LURE, Univ. Paris-Sud, BP 34, 91898 Orsay Cedex, France. Electronic address: lobo@lure.u-psud.fr

[1] N.L. Wang, A.W. McConnell, and B.P. Clayman, Phys. Rev. B **60**, 14 883 (1999).

[2] M.J. Rice and Y.R. Wang, Phys. Rev. B **36**, 8794 (1997).

[3] S.Y. Tian and Z.X. Zhao, Physica C **170**, 279 (1990).

[4] C.M. Varma, P.B. Littlewood, S. Schmitt-Rink, E. Abrahams, and A.E. Ruckenstein, Phys. Rev. Lett. **63**, 1996 (1989).

[5] J.C. Phillips, Phys. Rev. B **43**, 3656 (1991).

[6] J. Ruvalds and A. Virosztek, Phys. Rev. B **43**, 5498 (1991).

[7] E.G. Maksimov, Phys. Usp. **43**, 965 (2000).

[8] M. Ogata and P.W. Anderson, Phys. Rev. Lett. **70**, 3087 (1993).

[9] D.N. Basov, A.V. Puchkov, R.A. Hughes, T. Strach, J. Preston, T. Timusk, D.A. Bonn, R. Liang, and W.N. Hardy, Phys. Rev. B **49**, 12 165 (1994).

[10] A. Kapitulnik and G. Kotliar, Phys. Rev. Lett. **54**, 473 (1985).

[11] C. Huscroft and R.T. Scalettar, Phys. Rev. Lett. **81**, 2775 (1998).

[12] M.V. Sadovskii, Phys. Rep. **282**, 225 (1997).

[13] A.V. Puchkov, D.N. Basov, and T. Timusk, J. Phys.: Condens. Matter **8**, 10 049 (1996).

[14] C. Renner, B. Revaz, J.Y. Genoud, K. Kadowaki, and Ø. Fischer, Phys. Rev. Lett. **80**, 149 (1998).

[15] B. Wuyts, E. Osquiguil, M. Maenhoudt, S. Libbrecht, Z.X. Gao, and Y. Bruynseraede, Phys. Rev. B **47**, 5512 (1993).

[16] T. Ito, K. Takenaka, and S. Uchida, Phys. Rev. Lett. **70**, 3995 (1993).

[17] H. Alloul, T. Ohno, and P. Mendels, Phys. Rev. Lett. **63**, 1700 (1989).

[18] J. Fink, N. Nücker, H. Romberg, M. Alexander, M.B. Maple, J.J. Neumeier, and J.W. Allen, Phys. Rev. B **42**, 4823 (1990).

[19] A.P. Reyes, D.E. MacLaughlin, M. Takigawa, P.C. Hammel, R.H. Heffner, J.D. Thompson, and J.E. Crow, Phys. Rev. B **43**, 2989 (1991).

[20] D.P. Norton, D.H. Lowndes, B.C. Sales, J.D. Budai, B.C. Chakoumakos, and H.R. Kerchner, Phys. Rev. Lett. **66**, 1537 (1991).

[21] A.I. Liechtenstein and I.I. Mazin, Phys. Rev. Lett. **74**, 1000 (1995).

[22] C.H. Booth, F. Bridges, J.B. Boyce, T. Claeson, Z.X. Zhao, and P. Cervantes, Phys. Rev. B **49**, 3432 (1994).

[23] A.G. Sun, L.M. Paulius, D.A. Gajewski, M.B. Maple, and R.C. Dynes, Phys. Rev. B **50**, 3266 (1994).

[24] G.A. Levin, T. Stein, C.C. Almasan, S.H. Han, D.A. Gajewski, and M.B. Maple, Phys. Rev. Lett. **80**, 841 (1998).

[25] M. Merz, N. Nucker, E. Pellegrin, P. Schweiss, S. Schuppler, M. Kielwein, M. Knupfer, M.S. Golden, J. Fink, C.T. Chen, V. Chakarian, Y.U. Idzerda, and A. Erb, Phys. Rev. B **55**, 9160 (1997).

[26] R. Fehrenbacher and T.M. Rice, Phys. Rev. Lett. **70**, 3471 (1993).

[27] K. Takenaka, Y. Imanaka, K. Tamasaku, T. Ito, and S. Uchida, Phys. Rev. B **46**, 5833 (1992).

[28] H.L. Liu, M.A. Quijada, A.M. Zibold, Y.D. Yoon, D.B. Tanner, G. Cao, J.E. Crow, H. Berger, G. Margaritondo, L. Forró, O. Beom-Hoan, J.T. Markert, R.J. Kelly, and M. Onellion, J. Phys.: Condens. Matter **11**, 239 (1999).

[29] R. Buhleier, S.D. Brorson, I.E. Trofimov, J.O. White, H.U. Habermeier, and J. Kuhl, Phys. Rev. B **50**, 9672 (1994).

[30] C. Bernhard, T. Holden, A. Golnik, C.T. Lin, and M. Cardona, Phys. Rev. B **62**, 9138 (2000).

[31] R.P.S.M. Lobo, N. Bontemps, D. Racah, Y. Dagan, and G. Deutscher, Europhys. Lett. **55**, 854 (2001).

[32] J.W. Allen and J.C. Mikkelsen, Phys. Rev. B **15**, 2953 (1976).

[33] For a rather comprehensive review, see A.V. Puchkov, D.N. Basov, and T. Timusk, J. Phys.: Condens. Matter **8**, 10 049 (1996).

[34] Written this way, Ω_p is a pulsation in mks units measured in s^{-1}. Using the mks values for ϵ_0, e, m^* and the speed of light c and taking n in cm^{-3} one obtains the plasma frequency in cm^{-1} by $\Omega_p^2 = 10^{-4} n e^2/(2\pi c)^2 \epsilon_0 m^*$.

[35] J. Schützmann, B. Gorshunov, K.F. Renk, J. Münzel, A. Zibold, H.P. Geserich, A. Erb, and G. Müller-Vogt, Phys. Rev. B **46**, 512 (1992).

[36] K. Yoshida, Phys. Rev. B **60**, 9325 (1999).

[37] P.W. Anderson, K.A. Muttalib, and T.V. Ramakrishnan, Phys. Rev. B **28**, 117 (1983).

[38] M. Ma and P.A. Lee, Phys. Rev. B **32**, 5658 (1985).

[39] A. Kapitulnik and G. Kotliar, Phys. Rev. Lett. **54**, 473 (1985).

[40] A.V. Puchkov, T. Timusk, S. Doyle, and A.M. Hermann, Phys. Rev. B **51**, 3312 (1995).

[41] D.N. Basov, B. Dabrowski, and T. Timusk, Phys. Rev. Lett. **81**, 2132 (1998).

[42] J.J. McGuire, M. Windt, T. Startseva, T. Timusk, D. Colson, and V. Viallet-Guillen, Phys. Rev. B **62**, 8711 (2000).

[43] D.M. Eagles, R.P.S.M. Lobo, and F. Gervais, Phys. Rev. B **52**, 6440 (1995).

[44] S. Lupi, P. Maselli, M. Capizzi, P. Calvani, P. Giura, and P. Roy, Phys. Rev. Lett. **83**, 4852 (1999).

[45] T. Mertelj, D. Kuščer, M. Kosec, and D. Mihailovic, Phys. Rev. B **61**, 15 102 (2000).

[46] S. Tajima, N.L. Wang, N. Ichikawa, H. Eisaki, S. Uchida, H. Kitano, T. Hanaguri, and A. Maeda, Europhys. Lett. **47**, 715 (1999).

[47] M. Grüninger, D. van der Marel, A. Damascelli, A. Erb, T. Nunner, and T. Kopp, Phys. Rev. B **62**, 12 422 (2000).

[48] D. B. Tanner and T. Timusk, in *Physical Properties of High Temperature Superconductors III*, edited by D. M. Ginsberg (World Scientific, Singapore, 1992), pp. 363–469.

[49] Using a distribution of cutoff energies does not improve the fit, except for rounding the minimum observed between the two peaks. Our best results were obtained with Gaussian distributions with full widths at half maximum of 10 and 15 cm^{-1}. Remarking that the data resolution is 4 cm^{-1} these distributions are basically single peaks.

[50] As was shown by W.A. Little [Phys. Rev. **134**, A1416 (1964)] polarization of localized states can lead to attraction and superconductivity of the carriers. The large polarizability in our case occurs due to the large radius l. Qualitative estimates show that at electron-electron separation less than $l(l/\epsilon a_B)^{1/3}$ the attraction between electrons due to the polarization of the localized states is comparable or larger than their Coulomb repulsion (ϵ is the dielectric function, and a_B is the Bohr radius).

[51] Z. Zou, J. Ye, K. Oka, and Y. Nishihara, Phys. Rev. Lett. **80**, 1074 (1998).

[52] Z.G. Zou, J.H. Ye, K. Oka, and Y. Nishihara, J. Alloys Compd. **277**, 37 (1998).

[53] Y. Nishihara, Z. Zou, J. Ye, K. Oka, T. Minawa, H. Kawanaka, and H. Bando, Bull. Mater. Sci. **22**, 257 (1999).

[54] M. Muroi and R. Street, Physica C **314**, 172 (1999).